Journal of Organometallic Chemistry, 435 (1992) 299–310
Elsevier Sequoia S.A., Lausanne
JOM 22671

Preparation and crystal structures of the complexes (η^5-$C_5H_4CMe_2$-η^5-$C_{13}H_8$)MCl_2 (M = Zr, Hf) and their role in the catalytic formation of syndiotactic polypropylene

Abbas Razavi
Fina Research, Centre de Recherche du Groupe Petrofina, Zone Industrielle C, B-7181 Feluy (Belgium)

and Joseph Ferrara
Molecular Structure Corporation, College Station, TX 77640 (USA)

(Received December 3, 1991)

Abstract

The reactions of MCl_4 (M = Zr, Hf) with the dilithium salt of 2-cyclopentadienyl-2-fluorenylpropane in pentane solution give the complexes (η^5-$C_5H_4CMe_2$-η^5-$C_{13}H_8$)MCl_2. NMR and X-ray diffraction data show that there are η^5-bonded fluorenyl groups in these complexes. When activated with methylalumoxane both complexes catalyse the stereospecific polymerization of propylene to syndiotactic polypropylene.

Introduction

The dianions of compounds containing two cyclopentadienyl or indenyl groups connected by $(CH_2)_n$ ($n = 1$–3), Me_2Si or Et_2Si units have been much used as ligands for reactions with various transition metal compounds, especially Group 4 metal halides [1–10]. Some of the resulting organometallic compounds, in particular the bisindenyl derivatives, have interesting structural and catalytic properties [11]. We describe below the syntheses and properties of new asymmetric transition metal *ansa* complexes with a η^5-cyclopentadienyl and a η^5-fluorenyl moiety connected through an isopropylidene bridge [12].

Correspondence to: A. Razavi, 9 Rue de Flandre, B-7340 Paturage, Belgium.

Results and discussion

The bridged 2-cyclopentadienyl-2-fluorenylpropane (**1**) is produced quantitatively by the following reaction:

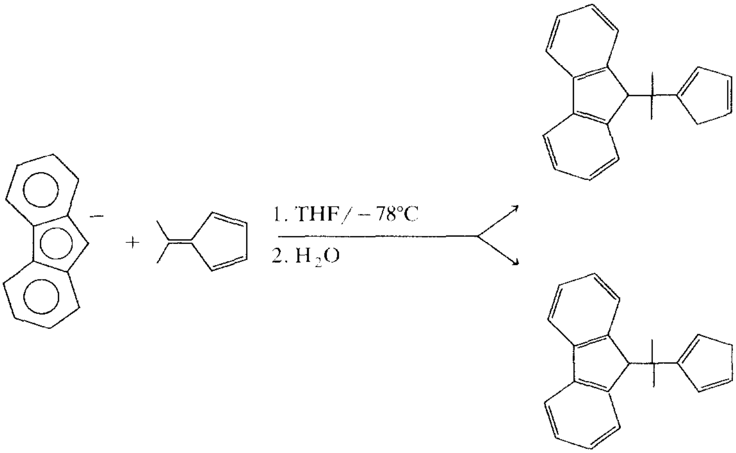

(**1**)

The ^{1}H NMR spectrum of **1** indicates the presence of two isomers. Double deprotonation of **1** with two equivalents of methyllithium in THF solution gives the corresponding dianion **2**.

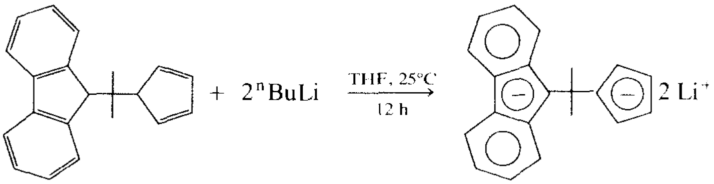

(**2**)

The reaction of **2** with one equivalent of MCl$_4$ in pentane yields the red complex **3** and the yellow complex **4**:

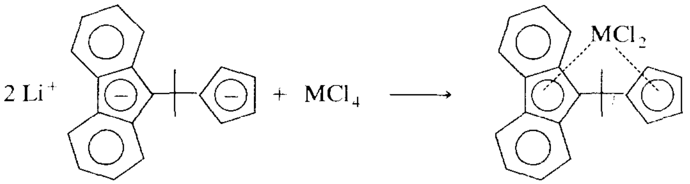

(M = Zr(**3**), Hf(**4**))

The identities of **3** and **4** have been confirmed by their ^{1}H NMR and mass spectra and their X-ray structures.

The ^{1}H NMR spectra of **3** and **4** in CD_2Cl_2 are almost identical; deviations are in the range of 0.01–0.06 ppm. Figure 1 shows the ^{1}H NMR spectrum of **3**.

The signals from the two methyl substituents in the bridge appear at $\delta = 2.35$ ppm. The two virtual triplets at δ 5.77 and 6.29 ppm result from an AA′BB′ pattern and are due to the protons in positions A and B in the C_5H_4 group. The two triplets at 7.27 and 7.55 ppm come from the protons in positions D and E, and

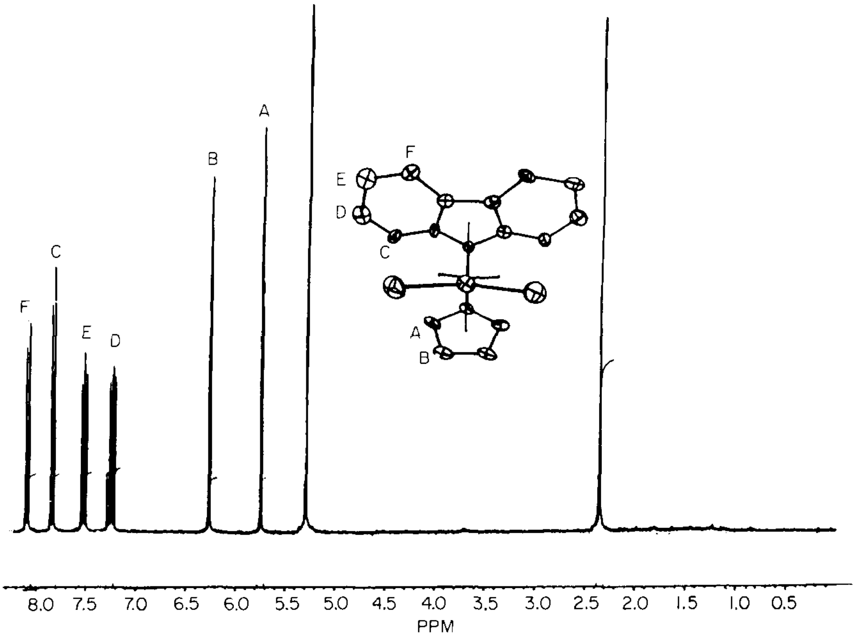

Fig. 1. ^1H NMR spectrum of 3 (300 MHz, in CD_2Cl_2, room temperature).

the two doublets at 7.87 and 8.12 ppm from the protons in positions C and F. The coupling constants in the doublets and triplets are *ca*. 8.4 Hz.

X-Ray structures of 3 and 4

The molecular structures of **3** and **4** are shown in Fig. 2. Important bond distances and angles are given in Table 1. Complexes **3** and **4** have almost identical structures and so only that of **3** is discussed. The angle at the isopropylidene carbon (C(1)–C(14)–C(17) = 99.4°) is much smaller than expected; this may be due to the metallocenophane character. The two centroid zirconium connections form a Flu–Zr–Cp angle (Flu = fluorenyl) of 118.6° at Zr. The Cl–Zr–Cl angle is 98.2°.

The progressive increase in the Zr–C bond distances from the bridgehead carbon C(1) (2.401(8)) to C(2) (2.501(8)), C(5) (2.528(8)), C(3) (2.665(7)) and C(4) (2.651(7)) would in itself be consistent with a η^3-bonded fluorenyl ring, but the increase is not large enough for this. Instead we believe that it is the nonbonding interaction between the two chloride ligands and the dorsal carbons of the two six-membered rings that gives rise to this variation in the bond distances. The thermal stability of **3** and **4** also favours the η^5-bonded structure. Similar reasoning applies to the Zr–C bond distances to the cyclopentadienyl moiety. The Zr–C(19) (2.519(8) Å) and Zr–C(20) (2.528(8) Å) distances are on average about 0.2 Å longer than the other three. Again the non-bonding contacts between the two chlorine atoms and the distal carbon and hydrogen atoms are responsible for the repulsion that gives rise to this bond lengthening. This is of prime importance for the stereoselectivity of the actual catalysts. These dorsal and distal positions of the cyclopentadienyl and the fluorenyl parts of the ligand lie exactly above and below the complexation sites of the monomer and the growing polymer chain. By

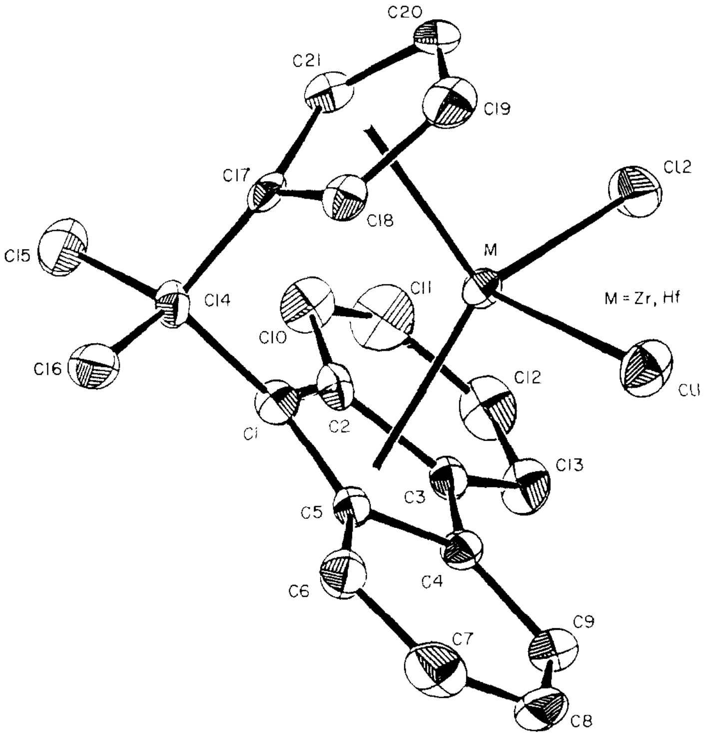

Fig. 2. Molecular structures of **3** and **4**.

interacting with their substituents they regulate the conformation of the growing chain and the prochiral face of the monomer to be complexed.

Polymerization behaviour

Complexes **3** and **4** are very active catalyst precursors for the homogeneous polymerization of α-olefins. When activated by methylalumoxane (MAO) or other ionizing agents **3** and **4** are able to promote the polymerization of propylene to give highly syndiotactic polypropylene. Complex **3** shows higher activity and stereospecifity than **4** [12].

Mechanistic aspects of the polymerization

The stereochemistry of the metallocene-based syndiospecific polymerization is governed by the stereorigid chiral environment of the transition metal. This so-called enantiomeric-site stereochemical control mechanism [13] implies that the chiral catalytic centres are capable of discriminating between the two prochiral (*re* and *si*) enantiofaces of a propylene molecule. However, whereas in the isospecific case the configuration of the catalytic complex remains unchanged (either *S* or *R*) throughout the polymerization, the configuration of the syndiotactic specific complex must change systematically from *R* to *S* and *vice versa* after each insertion step (site isomerization).

The prochiral complexes **3** and **4** have bilateral symmetry and the two chlorine substituents are mirror images with respect to a plane of symmetry bisecting the

Table 1

Bond lengths (Å) and bond angles (°) for **3** and **4**, with e.s.d.s [a]

	3	**4**		**3**	**4**
M(1)–C(1)	2.401(8)	2.391(6)	C(3)–C(4)	1.43(1)	1.46(3)
M(1)–Cl(1)	2.422(3)	2.394(6)	C(4)–C(9)	1.39(1)	1.38(3)
M(1)–Cl(2)	2.425(2)	2.40(2)	C(4)–C(5)	1.44(1)	1.44(2)
M(1)–C(17)	2.436(7)	2.41(2)	C(5)–C(6)	1.44(1)	1.41(3)
M(1)–C(18)	2.444(8)	2.44(2)	C(6)–C(7)	1.35(1)	1.34(3)
M(1)–C(21)	2.452(8)	2.46(2)	C(7)–C(8)	1.39(1)	1.43(3)
M(1)–C(2)	2.501(8)	2.49(2)	C(8)–C(9)	1.35(1)	1.43(3)
M(1)–C(19)	2.519(8)	2.50(2)	C(10)–C(11)	1.35(1)	1.34(3)
M(1)–C(20)	2.528(8)	2.51(2)	C(11)–C(12)	1.38(1)	1.42(3)
M(1)–C(5)	2.528(8)	2.57(2)	C(12)–C(13)	1.37(1)	1.34(3)
M(1)–C(4)	2.651(7)	2.64(2)	C(14)–C(17)	1.53(1)	1.55(3)
M(1)–C(3)	2.665(7)	2.64(2)	C(14)–C(15)	1.53(1)	1.55(3)
C(1)–C(5)	1.43(1)	1.45(2)	C(14)–C(16)	1.55(1)	1.57(2)
C(1)–C(2)	1.45(1)	1.49(3)	C(17)–C(18)	1.41(1)	1.36(3)
C(1)–C(14)	1.53(1)	1.57(2)	C(17)–C(21)	1.43(1)	1.44(3)
C(2)–C(10)	1.42(1)	1.39(2)	C(18)–C(19)	1.41(1)	1.41(2)
C(2)–C(3)	1.44(1)	1.41(3)	C(19)–C(20)	1.38(1)	1.35(3)
C(3)–C(13)	1.42(1)	1.41(3)	C(20)–C(21)	1.39(1)	1.38(2)
Cp–M–Flu	118.6	119.4			
Cp–Flu	72.0	70.0			
Cl(1)–M–Cl(2)	98.2	97.5			
C(1)–C(14)–C(17)	99.4	101.0			
C(15)–C(14)–C(16)	106.5	106.0			

[a] Cp = cyclopentadienyl centroid; Flu = fluorenyl centroid.

Cl–M–Cl angle (*cf.* Fig. 2). On the basis of our own experiments and recent literature [14] we assume that immediately after addition of the MAO solution to **3** or **4** a cation is formed as follows in a two-step process; first through chloride/alkyl exchange the metallocene is methylated, and the product then gives a cation as a result of abstraction of a methyl anion by the stronger Lewis acid sites of MAO.

Table 2

Polymerization results and conditions [a] for **3** and **4**/MAO

Complex	μmol	Pol. temp. (°C)	Time (min)	Activity (pol./g cat./h)	$M_w (\times 10^{-3})$	MWD [c]	r [d] (%)
3	1.3	50	25	194000	133	1.8	0.96
3	1.2	70 [b]	60	315000	108	2.4	0.93
4	9.2	50	30	54000	777	2.3	0.74
4	5.8	70	60	32000	474	2.6	n.d.

[a] Propylene (1.2 l); 10 ml of 10.7 mol.% MAO (Schering). [b] MAO (5 ml). [c] MWD = M_w/M_n = molecular weight dispersity. Ratio of weight average molecular weight (M_w) to number average molecular weight (M_n). [d] The racemic diad *r* consists of two adjacent monomer units with inverse relative configuration. Its percentage is defined as the syndiotacticity index (SI) and can be calculated from the triad and pentad intensities obtained from the methyl region of the ^{13}C NMR spectrum of the polymer using the following equations: $r = 1/2\ mr + rr$; $rr = mrrm + mrrr + rrrr$; $mr = mmrm + mmrr + rmrm + rmrr$. n.d. not determined.

This tricoordinated, coordinatively and electronically unsaturated cationic species subsequently undergoes coordination by a propylene molecule to form a pseudo tetrahedral chiral cationic complex which is stabilized by an MAO anion. The configuration of this cationic complex can be *R* or *S* depending on the position of the methyl group and the coordinated monomer, as shown below.

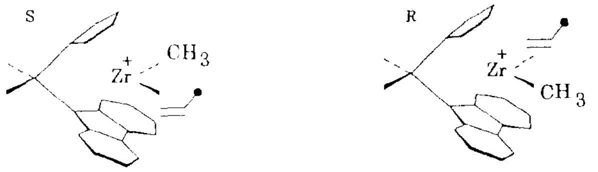

The cationic *S* and *R* enantiomers

Each of these enantiomers can discriminate between the two prochiral faces of the propylene and complex preferentially to one face. Owing to the chain-migratory nature of the insertion step [15] the growing polymer chain and the incoming monomer swap sites after each insertion, giving rise to continuous site isomerization that leads to alternate enchainment of monomer units with inverse relative configuration and the formation of a syndiotactic chain. The appearance of pairs of *meso* diads *mm* in an otherwise of long sequences of racemic diads consisting polymeric chain is a direct consequence of occasional coordination of a monomer with the wrong face, and is indicative of the enantiomorphic-site stereochemical control mechanism (Scheme 1).

The pentad distribution analysis of the ^{13}C NMR spectrum (Fig. 3(a)) of the polymer produced by **3** confirms the presence of the randomly distributed *mm* stereodefects as the predominant source of stereo irregularity in the polymer microstructure, and fully supports the proposed mechanism.

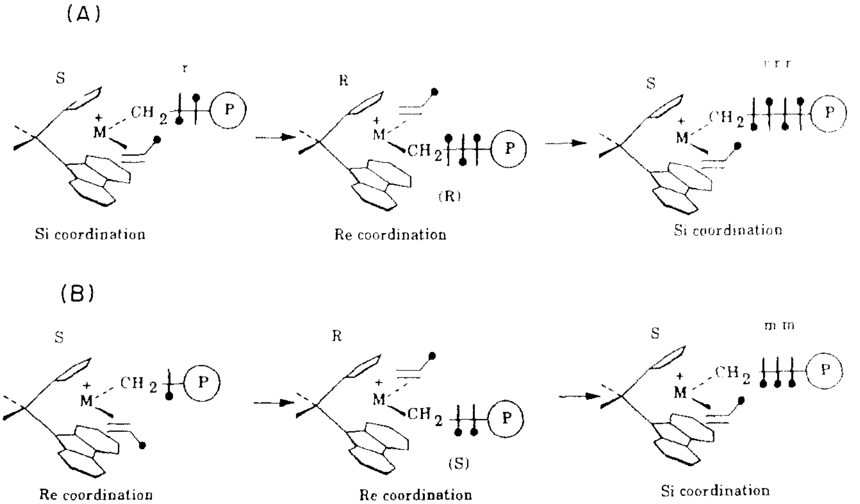

Scheme 1. (A) Enantiomorphic-site stereochemical control mechanism with chain migration for syndiotactic propagation. (B) Reverse enantio face selectivity and formation of *mm* stereodefects.

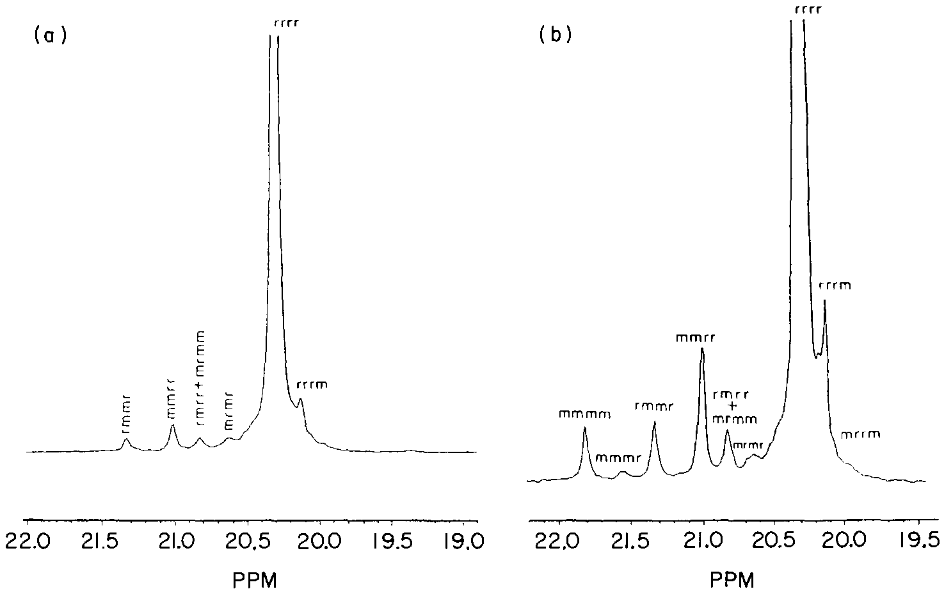

Fig. 3. The ^{13}C NMR spectra of the methyl pentad region of the syndiotactic polypropylene produced with (a) **3** at 50°C and (b) **4** at 30°C in combination with MAO. TMS scale.

The origin of the less frequent single *m* stereodefects is controversial: mechanisms involving processes such as classical chain end control, occasional skipped olefin insertion, and olefin insertion without chain migration in a site controlled mechanism [16], can theoretically account for their formation, but there is no convincing experimental evidence for such processes. In spite of their almost identical structures, **3** and **4** show some differences in their catalytic behaviour (Table 2). Complex **3** is about ten times the more active, and produces shorter but much more stereoregular polymer chains. Since the polymerization in both cases proceeds by the same mechanism, the reasons for the different behaviour of **3** and **4** must have thermodynamic and kinetic origins, and can be related to the difference in Zr–C and Hf–C bond strengths.

The activities of the catalysts and the molecular weights of the polymers are directly related to the balance of initiation, propagation, and termination reaction rates during the polymerization process. The weaker Zr–C (stronger Hf–C) bond results in a faster (slower) monomer insertion and higher (lower) propagation rate. Since the termination rate is related to β-H-elimination, it is higher for complex **3**, with the weaker M–C bond and shorter-lived transition states involving reversible β-H agostic intermediates [17–20]. The net effect is that **4** produces longer chains at slower rates and **3** produces shorter chains with higher rates. The effect of the M–C bond strength on the difference in the stereoregularity of the two polymers can be interpreted as follows. The stronger Hf–C bond with longer-lived H-agostic transition states, disfavours the chain migration, and so multiple insertion on the same site without chain migration can occasionally occur, leading to incorporation of short isotactic sequences in the syndiotactic backbone of the polymer. The ^{13}C NMR spectra of SPP produced by **4** (Fig. 3b) reveals the presence of short isotactic sequences as stereodefects in addition to the mm stereodefects, accounting for its lower stereoregularity.

Experimental

All operations were performed under an inert gas by glovebox or Schlenk techniques. Pentane and methylene chloride were dried over calcium hydride and toluene and tetrahydrofuran (THF) over sodium/benzophenone. All solvents were freshly distilled before use. $HfCl_4$ and $ZrCl_4$ were obtained from Comprehensive Research Chemical Corporation, P.O. Box 4591, Anaheim, CA, USA. The elemental analyses were performed by Galbraith Laboratories, Knoxville TN, USA.

2-Cyclopentadienyl-2-fluorenylpropane (1)

Fluorene (44 g, 0.25 mol) and THF (250 ml) were placed in a round-bottom flask equipped with side arm, addition funnel and magnetic stirring bar and an equimolar amount of methyllithium in diethyl ether (1.4 *M*) was added during 30 min at room temperature. The resulting deep red solution was stirred for several hours until gas evolution had completely ceased, and a solution of 26.5 g (0.25 mol) of 6,6-dimethylfulvene in THF (100 ml) was added dropwise. The red solution was stirred overnight and then treated with 200 ml of water. The mixture was stirred for 10 min and the organic layer then extracted several times with 100 ml portions of diethyl ether. The combined organic phases were dried over magnesium sulfate and the ether removed to leave a yellow solid, which yielded 64.6 g (95%) of a white product upon recrystallization from a chloroform/methanol mixture. The compound sublimes at 60°C under high vacuum, to give colourless needles, m.p. 91.4°C. Anal. Found: C, 91.90; H, 7.22. $C_{21}H_{20}$ calc.: C, 92.65; H, 7.35%. MS (EI, 10 eV), m/e 272 (M^+).

Preparation of the dianion 2

A 500 ml round-bottom flask equipped with a side arm, addition funnel and stirring bar was charged with 6.8 g (0.025 mol) of 2-cyclopentadienyl-2-fluorenylpropane in 200 ml of THF. To this solution two molar equivalents of n-butyllithium in hexane (1.6 *M*) were added dropwise at room temperature. The resulting red solution was stirred for 12 h, the THF then removed under vacuum, and the residue washed with pentane to give the dilithiated compound as a yellow powder in quantitative yield. The product was used without further purification.

Preparation of 3

To a suspension of 0.025 mol of **2** in 200 ml of dry pentane in a 1 l round-bottom flask equipped with a magnetic stirring bar was added a suspension of an equimolar amount of $ZrCl_4$ powder in 200 ml of pentane. The mixture was stirred for 6 h during which the suspension became red and the reaction went to completion. The pentane was decanted and the remaining red solid was extracted with methylene chloride (to leave behind LiCl). Cooling of the extract to −20°C gave analytically-pure red crystals in quantitative yield. MS: $m/e = 133$ (M^+);

Anal. Found: C, 58.06; H, 4.14; Cl, 16.34; Zr, 20.99. $C_{21}H_{18}Cl_2Zr$ calc.: C, 58.17; H, 4.19; Cl, 16.34; Zr, 20.07%.

Preparation of 4

An identical procedure to that used for **3**, but starting from Hf–Cl_4 (and giving a lemon-yellow product suspension) yielded analytically pure yellow crystals in

Table 3

Positional parameters and B_{eq} for **3**

Atom	x	y	z	B_{eq}
Hf(1)	0.17256(8)	0.1792(1)	0.61798(5)	1.58(3)
Cl(1)	0.2198(5)	0.0148(6)	0.5245(3)	2.5(2)
Cl(2)	0.0548(5)	0.0026(6)	0.6768(3)	2.5(2)
C(1)	0.317(2)	0.369(2)	0.676(1)	1.6(4)
C(2)	0.290(2)	0.278(2)	0.737(1)	1.3(4)
C(3)	0.348(2)	0.137(2)	0.737(1)	1.7(4)
C(4)	0.415(2)	0.134(2)	0.675(1)	1.7(4)
C(5)	0.403(2)	0.278(2)	0.639(1)	1.2(4)
C(6)	0.460(2)	0.297(2)	0.577(1)	3.0(5)
C(7)	0.534(2)	0.187(3)	0.557(1)	2.3(4)
C(8)	0.554(2)	0.046(2)	0.594(1)	2.0(4)
C(9)	0.488(2)	0.020(2)	0.653(1)	2.2(4)
C(10)	0.218(2)	0.303(2)	0.792(1)	2.6(4)
C(11)	0.209(2)	0.196(3)	0.842(1)	2.9(4)
C(12)	0.272(2)	0.056(3)	0.842(1)	3.2(5)
C(13)	0.338(2)	0.023(2)	0.789(1)	2.5(4)
C(14)	0.245(2)	0.516(2)	0.646(1)	2.1(4)
C(15)	0.215(2)	0.623(2)	0.707(1)	3.0(5)
C(16)	0.323(2)	0.612(2)	0.600(1)	2.9(4)
C(17)	0.121(2)	0.448(2)	0.599(1)	1.5(4)
C(18)	0.025(2)	0.384(2)	0.628(1)	1.7(4)
C(19)	−0.044(2)	0.288(2)	0.575(1)	1.5(4)
C(20)	0.012(2)	0.286(2)	0.515(1)	1.5(4)
C(21)	0.118(2)	0.377(2)	0.529(1)	2.3(4)
H(1)	0.4468	0.3870	0.5487	3.6
H(2)	0.5744	0.2046	0.5166	2.8
H(3)	0.6090	−0.0277	0.5797	2.5
H(4)	0.4943	−0.0744	0.6776	2.6
H(5)	0.1748	0.3963	0.7939	3.2
H(6)	0.1593	0.2158	0.8783	3.5
H(7)	0.2672	−0.0157	0.8791	3.9
H(8)	0.3767	−0.0725	0.7862	3.0
H(9)	0.2929	0.6563	0.7359	3.6
H(10)	0.1685	0.7074	0.6849	3.6
H(11)	0.1663	0.5706	0.7366	3.6
H(12)	0.3984	0.6482	0.6302	3.4
H(13)	0.3454	0.5520	0.5617	3.4
H(14)	0.2730	0.6953	0.5789	3.4
H(15)	0.0078	0.4010	0.6759	2.0
H(16)	−0.1189	0.2339	0.5797	1.8
H(17)	−0.0166	0.2312	0.4713	1.8
H(18)	0.1794	0.3901	0.4982	2.8

quantitative yield. MS: $m/e = 522$ (M^+); Anal. Found: C, 48.39; H, 3.45; Cl, 13.59; Hf, 34.11. $C_{21}H_{18}Cl_2H$ calc.: C, 48.79; H, 3.40; Cl, 15.14; Hf, 33.20%.

*X-Ray data collection, solution and refinement of **3** and **4***

Crystal data for $C_{21}H_{18}Cl_2Hf$, $M = 519.77$. Monoclinic space group $P2_1/c$ (No. 14), a 10.66(1), b 8.878(5), c 18.59(2) Å, β 100.51(9)°, V 1729(3) Å^3, $Z = 4$, d_{calc}

Table 4

Positional parameters and B_{eq} for **4**

Atom	x	y	z	B_{eq}
Zr(1)	0.24342(6)	0.21497(9)	0.46572(5)	2.10(3)
Cl(1)	0.2682(2)	0.0377(3)	0.5841(2)	3.9(1)
Cl(2)	0.1959(2)	0.0524(3)	0.3417(2)	3.8(1)
C(1)	0.1744(6)	0.4524(9)	0.4853(5)	2.4(4)
C(2)	0.1070(6)	0.3981(8)	0.4083(5)	2.3(3)
C(3)	0.0374(5)	0.289(1)	0.4387(5)	2.4(3)
C(4)	0.0618(6)	0.274(1)	0.5334(5)	2.4(3)
C(5)	0.1429(6)	0.3794(9)	0.5616(5)	2.1(4)
C(6)	0.1741(7)	0.387(1)	0.6565(6)	3.2(4)
C(7)	0.1280(9)	0.297(1)	0.7120(6)	4.6(5)
C(8)	0.0502(8)	0.196(1)	0.6823(6)	4.2(5)
C(9)	0.0171(7)	0.186(1)	0.5939(6)	3.5(4)
C(10)	0.0954(7)	0.427(1)	0.3148(6)	3.5(4)
C(11)	0.0202(8)	0.357(1)	0.2601(6)	4.6(5)
C(12)	−0.0475(7)	0.256(1)	0.2903(6)	4.3(5)
C(13)	−0.0387(6)	0.217(1)	0.3786(6)	3.5(4)
C(14)	0.2742(6)	0.5461(8)	0.4801(5)	2.3(3)
C(15)	0.2650(7)	0.660(1)	0.4065(7)	4.0(4)
C(16)	0.3100(7)	0.626(1)	0.5689(6)	3.9(4)
C(17)	0.3552(6)	0.4289(8)	0.4635(5)	2.3(4)
C(18)	0.4071(6)	0.336(1)	0.5287(6)	2.7(4)
C(19)	0.4453(6)	0.213(1)	0.4871(7)	4.0(4)
C(20)	0.4181(6)	0.228(1)	0.3963(6)	3.2(4)
C(21)	0.3624(7)	0.356(1)	0.3803(6)	2.9(4)
H(1)	0.2266	0.4543	0.6800	3.9
H(2)	0.1497	0.3030	0.7744	5.5
H(3)	0.0206	0.1343	0.7239	5.1
H(4)	−0.0366	0.1178	0.5732	4.2
H(5)	0.1406	0.4956	0.2909	4.2
H(6)	0.0138	0.3787	0.1980	5.6
H(7)	−0.1011	0.2130	0.2494	5.2
H(8)	−0.0825	0.1429	0.3989	4.2
H(9)	0.2064	0.7222	0.4140	4.8
H(10)	0.3293	0.7150	0.4100	4.8
H(11)	0.2537	0.6148	0.3497	4.8
H(12)	0.2513	0.6791	0.5869	4.6
H(13)	0.3333	0.5577	0.6139	4.6
H(14)	0.3672	0.6895	0.5602	4.6
H(15)	0.4152	0.3540	0.5913	3.2
H(16)	0.4827	0.1344	0.5162	4.8
H(17)	0.4347	0.1617	0.3518	3.8
H(18)	0.3336	0.3905	0.3232	3.4

1.996 g cm^3, $F(000) = 1000$, $\mu(\text{Mo-}K_\alpha)$ 62.89 cm^{-1}. Yellow, plate-shaped crystals suitable for X-ray diffraction analyses were grown from methylene chloride at −15°C. The crystal used for the study (maximum dimension 0.200 × 0.150 × 0.070 mm) was mounted on a glass fibre. Data collection was performed with graphite monochromated Mo-K_α radiation ($\lambda = 0.71060$ Å) on a Rigaku AFC6R diffractometer at −115°C. A total of 3298 unique reflections were measured ($+h$, $+k$, $+l$, ω scan mode 2θ max. = 50.2). An empirical absorption correction was applied by use of the program DIFABS and this resulted in transmission factors ranging from 0.73 to 1.27.

The structure was solved by direct methods (MITHRIL) expanded with the program DIRDIF [21] and refined by full matrix-least-squares:

$$\text{(function minimized)};\ \Sigma w(|F_o| - |F_c|)^2 \text{ with } w = \frac{4F_o^2}{[\sigma(F_o^2)]^2}$$

The hafnium and chlorine atoms were refined anisotropically and the carbon atoms isotropically. Hydrogen atoms were included in the structure factor calculation in calculated positions (dC–H = 0.95 Å), and were assigned isotropic thermal parameters 1.2 times those of the carbon to which they were bonded. The final agreement factors were $R = 0.058$ and $R_w = 0.060$ for 3298 reflections having $I > 3.00\ \sigma(I)$. The atomic coordinates are listed in Table 3.

The structure of **3** is very similar to that of **4**. $C_{21}H_{18}Cl_2Zr$, $M = 432.50$. Space group $P2_1/n$ (non-standard no. 14), a 12.544(2), b 9.298(1), c 15.031(2) Å, β 96.11(1)°, V 1743.2(5) Å^3, $Z = 4$, d_{calc} 1.648 g cm^{-3}. Refinement on the 1568 reflections with $I > 3.0\sigma(I)$ resulted in the residuals $R = 0.043$ and $R_w = 0.044$.

4: $C_{21}H_{18}Cl_2Hf$, $M = 519.77$. Space group $P2_1/c$ (No. 14), a 10.66(1), b 8.878(5), c 18.59(2) Å, β 100.51(9)°, V 1729.3 Å^3, $Z = 4$, d_{calc} 1.996 g cm^{-3}. Refinement on the 1614 reflections with $I > 3.0\sigma(I)$ resulted in the residuals $R = 0.058$ and $R_w = 0.060$. The atomic coordinates are listed in Table 4.

It is noteworthy that in spite of having virtually identical molecular structures **3** and **4** crystallize in different unit cells. It is possible that each can exist in two crystal forms, and that one of these separated for **3** and the other for **4**.

References

1 J.A. Smith, J. Seyerl, G. Huttner and H.H. Brintzinger, J. Organomet. Chem., 173 (1979) 175.
2 C.H. Saldarriga-Molina, A. Clearfield and I. Bernal, J. Organomet. Chem., 80 (1974) 79.
3 E.F. Epstein and I. Bernal, Inorg. Chim. Acta, 7 (1973) 211.
4 E. Marechal and A. Lapert, Bull. Soc. Chim. Fr., (1967) 2954.
5 J.A. Ewen, L. Haspeslagh, J.L. Atwood and H. Zhang, J. Am. Chem. Soc., 109 (1987) 6544.
6 H. Schwemlein and H.H. Brintzinger, J. Organomet. Chem., 254 (1983) 69.
7 F. Wochner, L. Zsolnai, G. Huttner and H.H. Brintzinger, J. Organomet. Chem., 288 (1985) 69.
8 C.S. Bajgur, W.R. Tikkanen and J.L. Petersen, Inorg. Chem., 24 (1985) 2539.
9 F.R.W.P. Wild, L. Zsolnai, G. Huttner and H.H. Brintzinger, J. Organomet. Chem., 232 (1982) 233.
10 A. Kabi-Satpathy, C.S. Bajgur, K.P. Reddy and J.L. Petersen, J. Organomet. Chem., 364 (1989) 105.
11 W. Kaminsky, K. Kulper, H.H. Brintzinger and F.R.W.P. Wild, Angew. Chem., Int. Ed. Engl., 24 (1985) 507.
12 J.A. Ewen, R.L. Jones, A. Razavi and J.D. Ferrara, J. Am. Chem. Soc., 110 (1988) 6255.
13 R.A. Sheldon, T. Fueno, T. Tsunesugu and J. Furukawa, J. Polym. Sci., 3 (1965) 23.

14 R.F. Jordan, C.S. Jajgur, R. Willett and B. Scott, J. Am. Chem. Soc., 108 (1986) 7410; G.G. Hlatky, H.W. Turner and R.R. Eckman, J. Am. Chem. Soc., 111 (1989) 2728; A. Razavi and U. Thewalt, to be published.

15 P. Cossee, Tetrahedron Lett., 17 (1960) 12.

16 A. Zambelli, C. Pellechia and L. Oliva, Makromol. Chem. Macromol. Symp., 48/49 (1991).

17 W. Röll, H.H. Brintzinger, B. Rieger and R. Zolk, Angew. Chem., Int. Ed. Engl., 29 (1990) 339.

18 H. Krauledat and H.H. Brintzinger, Angew. Chem., Int. Ed. Engl., 29 (1990) 1459.

19 B.J. Burger, M.E. Thompson, W.D. Cotter and J.E. Bercaw, J. Am. Chem. Soc., 112 (1990) 1566.

20 R.F. Jordan, P.K. Bradley, N.C. Baenziger and R.E. LaPointe, J. Am. Chem. Soc., 112 (1990) 1289.

21 Structure Solution Methods: MITHRIL – C.J. Gilmore, MITHRIL – an integrated direct methods computer program, J. Appl. Cryst. 17, 42–46, University of Glasgow, Scotland, (1984).
DIRDIF – P.T. Beurskens, DIRDIF: Direct Methods for Difference Structures – an automatic procedure for phase extension and refinement of difference structure factors. Technical Report 1984/1 Crystallography Laboratory, Toernooiveld, 6525 Ed Nijmegen, Netherlands.